RSC Advances

ROYAL SOCIETY OF CHEMISTRY

www.rsc.org/advances

Graphical Abstract

Acoustical method shows its ability to study the structure, energetics and spectroscopic aspects of charge transfer complexes of three different benzenoid compounds namely chlorobenzene (**1**), phenol (**2**) and anisole (**3**) with iodine and supported by UV-Visible and DFT methods.

1   **ULTRASONIC, SPECTROPHOTOMETRIC AND THEORETICAL**
2   **STUDIES OF SIGMA AND PI INTERACTIONS OF IODINE WITH**
3   **SUBSTITUTED BENZENE†**
4

5   *A. Justin Adaikala Baskar[a], R. Kumar[b], R. Vijay Solomon[c], Mahesh Sundararajan[d]*,*
6   *Venu Kannappan[e,]*, D. Roop Singh[e], M. Jaccob[a,]**
7

8   [a]Department of Chemistry, Loyola College, Chennai 600 034, Tamil Nadu, India
9   [b]Department of Physics, The New College, Chennai 600 014, Tamil Nadu, India
10 [c]Department of Chemical Engineering, University of South Carolina, Columbia, USA
11 [d]Theoretical Chemistry Section, Bhabha Atomic Research Centre, Mumbai 400 085, India
12 [e]Department of Chemistry, Presidency College, Chennai 600 005, Tamil Nadu, India
13

14   **Abstract**

15 The charge transfer (CT) interaction between the three structurally different benzenoid
16 compounds (donors), chlorobenzene (**1**), Phenol (**2**), Anisole (**3**) and iodine (I_2, acceptor) were
17 investigated by experimental methods (ultrasonic and UV-Visible analysis) and theoretical
18 calculations. Notably, strong solute − solute interaction and existence of CT type of interaction
19 between **1-3** and I_2 is clearly analyzed from the trend in acoustical and excess thermo acoustical
20 parameters with concentration at 303 K in n-hexane medium. The formation of 1:1 complexes
21 between iodine and **1-3** was established by UV–visible spectroscopic method. The structure and
22 stabilization energies of **1-3** and I_2 were further calculated by DFT calculations. Among the σ-
23 and π-type interactions, a π-type complex (**1a-3a**) with atom-centered orientation is found to be a
24 preferred and stable geometry for all CT complexes. The stability constant of the CT complexes
25 was calculated by spectroscopic and ultrasonic methods which show similar trend with DFT
26 computed stabilization energies, Further, AIM and NBO analysis was used to quantify the nature
27 of stabilizing interactions existing in **1-3** and I_2 CT complexes. Our computed results are in good
28 agreement with the experimental observations.

29

30

31

1 **1 Introduction**:

2   The directional non-covalent interactions between donors and acceptors such as halogens

3 are inevitable in the context of frontier areas of research including crystal engineering, drug

4 designing, and protein–ligand complexation.[1-3] These complexes have been identified as

5 potential candidates for non-linear optical materials and electrical conductivity.[4] In 1863,

6 Guthrie and coworkers have first reported that charge transfer (CT) complexes between ammonia

7 and iodine ($NH_3 \ldots I_2$) systems.[5] Charge-transfer interactions (CT) are the special kind of non-

8 covalent interaction which are ubiquitous in nature and are of much important in many biological

9 processes. Over the years, benzene-I_2 system have considered as a classical case of CT type

10 interactions. Later, Hilderband[6] reported the absorption characteristics of benzene-iodine CT

11 complexes. Further, the formation of CT complexes was investigated by Mülliken through

12 resonance model through spectroscopic and dipole moment studies.[7-8] Subsequently, significant

13 number of reports on spectroscopic and theoretical studies reveal that the geometry of CT

14 complexes between benzene and electrophilic halogens.[9-11] Notably, Fredin[12-13] and Ferguson[14-15]

15 have suggested that the existence of axial structure of benzene-iodine CT complexes in a

16 nitrogen matrix through IR experiments.

17   In conjunction to experimental measurements, electronic structure calculations[16-17] have

18 performed over the years to determine the most stable geometry conformation of benzene-iodine

19 CT complexes. Both density functional theory (DFT) based calculations (commonly B3LYP

20 functional is used) and "*ab initio* CCSD(T)" calculations by Mebel *et al*[18] have pointed out that

21 the most stable geometry for benzene-iodine CT complexes was above-bond conformation and

22 not the axial type. Besides, photo dissociation dynamics study of benzene-iodine complexes in

23 benzene solution by CT band resonance Raman spectra combined with DFT calculations showed

24 that atom-center-oriented geometry was found to be an active geometry in its CT excitation

25 states.[19] In addition to that, combined UV-PES and *ab initio* molecular orbital studies of

26 Venuvanalingam and coworkers have clearly explained the possibility of existence of most stable

27 bond centered oblique structure of benzene-iodine monochloride (ICl) CT complexes.[20]

28   Ultrasonic investigations of binary and ternary liquid mixtures, being convenient and

29 non-destructive methods and having much significance in assessing the nature of molecular

30 interactions in liquid mixtures.[21-24] But in recent years, the acoustical investigations have been

31 successfully employed in the detection, determination of stability constants and thermodynamic

1   properties of several CT and hydrogen bonded complexes.[25-28] Spectroscopic techniques have

2   been employed extensively to determine the equilibrium constant and extinction co-efficient (ε)

3   of CT complexes by several authors. The effect of the substituents on the aromatic moiety on

4   stability of these complexes has been studied by using the IR, NMR and UV- visible spectral

5   techniques.[29-30] The formation of CT complexes between iodine as σ-acceptor with certain

6   heterocyclic compounds have been investigated by ultrasonic and UV–visible spectral methods

7   in DMSO medium by Ulagendran et al.[31] They found that both UV- visible and ultrasonic

8   methods yielded similar association constant values for CT complexes.

9   Iodine is a good example for an acceptor species among halogens for CT interactions

10   with electron rich benzenoid compounds and it has biological applications.[32] In order to

11   understand the stability and orientational aspects of CT complexes of I_2 with benzenoid

12   compounds, three systems have chosen. To understand the orientation of electrophilic iodine on

13   the aromatic ring with respect to the different substituents is comprehensively addressed from

14   experiment and theory by considering phenol$\cdots$I$_2$, anisole$\cdots$I$_2$ and chlorobenzene$\cdots$I$_2$ systems. The

15   notable feature of our work is the applications of ultrasonic scan in the ternary systems in the

16   detection of CT complexes and determination of their stability constants. Thermo-acoustic and

17   excess thermo-acoustical properties are reported in support of formation of these complexes.

18   Often in the acoustical method, Marwein-Bhatt equation[33] is used to calculate the stability

19   constants. However, this method is suitable for relatively strong CT complexes and moreover the

20   formation constants obtained by this method is concentration dependent. In the present work,

21   Kannappan equation[31b] was utilized to determine the concentration independent stability constant

22   and thermodynamic properties of such weak complexes. The spectral and theoretical methods are

23   used as supportive methods. Interestingly, our present work comprehensively compares the

24   structural, stability, bonding and spectral aspects of classical and halogen bonded complexes of

25   chlorobenzene, phenol and anisole with iodine using the acoustic method along with UV-Visible

26   and theoretical methods (AIM, NBO & TDDFT).

27

28   **2 Materials and Method**

29   The MERCK AR grade of iodine, chlorobenzene (**1**), phenol (**2**), anisole (**3**) and

30   n-hexane were purchased from S D fine chemicals, India. Iodine was purified by sublimation and

31   **1-3** were distilled before use in order to achieve higher purity. The density, (ρ) of the pure

liquids and their ternary systems were determined accurately by using a 10 ml specific gravity

bottle. The ultrasonic velocities in pure liquids and their ternary liquid mixtures were measured

with an accuracy of 0.1 ms^{-1} using a single crystal variable path ultrasonic interferometer

operating at 2 MHz frequency. Viscosity measurements were made with an Ostwald's

viscometer in which the flow time for solutions were measured through a digital stop clock of

accuracy ± 0.01s. The temperature of the samples was maintained at 303 K by digitally

controlled thermostatic water bath. Electronic absorption spectra of the samples were recorded in

PERKIN ELMER LAMDA 25 model spectrophotometer provided with thermostatic control at

303 K. Stability constants of the CT complexes of **1-3** with iodine are determined from the slope

and intercept of Benesi–Hildebrand (B-H) plots.

2.1 Method of calculation for acoustical parameters:

The various acoustical and excess thermo acoustical parameters were calculated from the

measured values of ultrasonic velocity (u), density (ρ) and viscosity (η) using the standard

formulae.[24,31b] Isentropic compressibility (κ_s) can be calculated from ultrasound speed and

density for a given solution at a given temperature using the equation (1):

$$\kappa_s = (u^2\rho)^{-1} \tag{1}$$

The following equations (2-4) are used to calculate free length (L_f), internal pressure (π_i),

and specific acoustic impedance (Z):

$$L_f = K_T\kappa_s^{1/2} \tag{2}$$

K_T is temperature dependent constant. Its value is $(93.875 + 0.375\ T) \times 10^{-8}$

$$\pi_i = bRT\ (K\eta/u)^{1/2}\rho^{2/3} / M_{eff} \tag{3}$$

$$Z = u\ \rho \tag{4}$$

In the above equations, effective molecular weight is calculated from mole fraction (x_i)

and molecular weight (M_i) of pure component 'i' using the equation $M_{eff} = \sum_i x_i M_i$; and b is a

constant. Its value is 2; R is universal gas constant; K is temperature independent constant which

is equal to 4.28×10^9 for all liquids, u is ultrasonic velocity and ρ is the measured density.

The excess thermoacoustic parameter is defined as the difference between the

experimental and ideal mixture values. It is a measure of the non – ideal behaviour of the system

as a consequence of associative or of other interactions. Excess thermo acoustic property (Y^E) is

obtained using the following general equation:

1 $$Y^E = Y - \sum_i (x_i y_i) \tag{5}$$

2 Where, Y is the experimental thermo acoustic property; x_i is mole fraction of ith component and

3 y_i is the thermo acoustic property of pure component i.

4   Marwein and Bhatt[33] proposed an equation to calculate the stability constants of donor-

5 acceptor complexes in binary liquids. Their equation generally gives concentration dependent

6 formation constant and it can be used only for relatively stable and strong complexes. Recently,

7 Kannappan et. al.[31b] have proposed an equation to calculate the formation constant values of the

8 charge transfer complexes, appreciable especially to weak complexes and in very dilute

9 solutions. The equilibrium constant for 1:1 stoichiometric reaction is calculated from the

10 ultrasonic velocity using Kannappan equation[41] as follows

11 $$K = y / (b-y)^2 \tag{6}$$

12 Here, $\qquad\qquad\qquad\qquad y = (a-k^{1/2} b) / (k - k^{1/2})$

13 Where $k = x/y$, x is the difference between u_{cal} and u_{obs} at lower concentration 'a', y is the

14 difference between u_{cal} and u_{obs} at higher concentration 'b'. u_{cal} is the ultrasonic velocity of the

15 mixture calculated from the mole fraction of the components using additive principle.

16 **2.2 Computational Details:**

17   Quantum chemical calculations were carried out using Gaussian 09[34] and Orca 3.0[35]

18 program. The CT complexes were optimized at BP86[36-37] functional in combination with

19 Grimme's D3 dispersion correction[38] using def2-TZVP for carbon, hydrogen and segmented all

20 electron relativistically contracted (SARC) for iodine atom. Followed by structural optimization,

21 vibrational frequencies were computed to confirm the stationary points as well as to identify the

22 unrealistic saddle points. Relativistic effects are incorporated using ZORA. B3LYP[39] with def2-

23 TZVP basis set (for iodine, all electrons scalar relativistic basis set (SARC)[40]) was used to carry

24 out the single point energy calculation. All interaction energy calculations were corrected for the

25 basis set superposition error (BSSE) utilizing counterpoise correction.[41] We find that the

26 computed BSSE (using BP86/def2-TZVP) is less than 3 kJ mol^{-1} thus the total binding affinity is

27 unaltered. Thus the computed binding free energies are BSSE uncorrected. In addition to the gas

28 phase calculations, influence of solvent on the CT complex formation was considered by

29 carrying out conductor like screening model (COSMO)[42] method in n-hexane (ε=1.89). Time

30 dependent density functional theory (TDDFT[43]) and natural bond orbital analysis (NBO[44-45])

31 calculations were carried out using G09. Here, ω-B97X-D3[46] with 6-311++G(d,p) basis set for

1　other atoms and SDB-aug-cc-pVQZ[47a] basis set for iodine atom was used to carry out the NBO

2　analysis and TD-DFT calculations. Solvent effects on the absorption spectra were evaluated on

3　the gas phase optimized geometries with n-hexane, using the SCRF-PCM method.[47b-d] First 20

4　roots were considered in the TD-DFT calculations. Bader's topological analysis is performed

5　using AIM2000 software.[48] B3LYP/6-311++g(d,p) level is used to generate the necessary wave

6　functions for the topological analysis.

7　**3 Results and Discussion:**

8　**3.1 Acoustical analysis**

9　　　　The ultrasonic velocity (u), density (ρ) and viscosity (η) for the ternary systems (**1-3**) are

10　summarized in Table 1. The plot of ultrasonic velocity (u) against concentration for **1-3** is

11　presented in Figure 1. It is clear from the plots in Figure 1(a) and data in Table 1, ultrasonic

12　velocity increases with increasing the concentration of components in all the three ternary

13　systems. It is observed that the increase is not perfectly linear with concentration in the three

14　systems. Similar type of variation in 'u' in **1** to **3** suggests the existence of same type of

15　interaction in all the three systems. The solute-solvent interaction in these ternary systems is less

16　prominent since chemically inert and non-polar n-hexane is employed. Hence, increase in

17　ultrasonic velocity with increasing the concentration is largely associated with the solute-solute

18　interaction of unlike molecules.[49] It is well known that phenol is an associated liquid and the

19　association occurs through strong intermolecular hydrogen bond.[50] The increase in 'u' is steeper

20　above 0.004M and this suggests that there is a rupture of hydrogen bonding of like ones at this

21　concentration and above this concentration specific interaction between the unlike molecules

22　appears to be dominant. Similar trend is also observed for the variation of density in **2**.

23　　　　Plots of isentropic compressibility vs concentration are given in Figure 1(b). Isentropic

24　compressibility'κ_s' is found to decrease with increasing the concentration in **1-3** which is the

25　reverse trend as that of ultrasonic velocity (Table 2). The decrease in isentropic compressibility

26　(κ_s) in liquid mixtures indicates that there is a definite contraction on mixing and the

27　considerable variation is attributed to strong interaction such as complex formation involving CT

28　complexes.[51] Compressibility changes with structure which leads to the change in ultrasonic

29　velocity. It is seen that the decrease in 'κ_s' is significant in **2** above 0.006M and this also shows

30　that the structure breaking behaviour in **2** is dominant in very dilute solution (<0.006 M) and the

31　non-covalent CT complex formation is dominant above this concentration. The variation of

ultrasonic velocity (u) is predominately determined by another important acoustical parameter intermolecular free length (L_f). Intermolecular free length (L_f) reflects similar behaviour as isentropic compressibility(κ_s) in such a way that there is a regular decrease in L_f with increase in concentration in all the three systems. The decrease in compressibility brings the molecules to close packing, resulting in the decrease of intermolecular free length. Decrease in intermolecular free length leads to positive deviation in sound velocity and negative deviation in compressibility. L_f values are computed for the **1-3** at 300K and listed in Table **2**. It is observed that there is decrease in L_f value with concentration in the three systems. This clearly indicates that closer proximity of the unlike molecules in the ternary systems. Further, the trend in L_f value with concentration is similar to the trend in κ_s values in the three systems It is interesting to note that 'L_f' value in **2** increases in very dilute solution and then decreases with increase in concentration as in other two systems. This suggests that there is structure breaking of associated phenol by solvent molecules and then only complex formation occurs.[52,21] The combination of structure breaking behaviour and charge transfer complex formation between I_2 and **2** is clearly supported by strong solute-solute interaction in the ternary mixtures. This is also supported by the internal pressure (π_i) values (Table 2). In **2**, π_i value is slightly higher in very dilute solution, decreases up to 0.006 M and thereafter it remains constant. This suggests that the structure breaking property is dominant up to this concentration of 0.006M. Above the concentration range, the complex formation is significant.[53] This kind of behaviour is not obtained in the case of **1** and **3**. At the same concentration range, L_f remains a constant in the case of **1** and **3**. It may be pointed out that above 0.006M concentration the π_i values are in the following order: **3** > **2** > **1**. This trend clearly suggests that the CT complex formation is significant above this concentration.

In order to confirm the existence of non-covalent interactions between the donor and acceptor, the excess values of the acoustical parameters such as κ_s, L_f and acoustic impedance (Z) were calculated. The sign and magnitude of excess ultrasound speed (u^E) play a prominent role in describing a molecular interactions occurring among the molecules of components in liquid mixtures. Any non-zero value in excess parameter is a measure of non-linearity and indicative of the existence of strong non-covalent interaction among the components of the systems.[25-26] The negative value of excess adiabatic compressibility indicates a strong attractive interaction are likely to occur between the components, while for mixtures with only weak

London type interactions possesses a positive value of excess adiabatic compressibility.[27-28] It is found that the u^E values (Table 2) are positive for **1-3** over the entire range of concentration [Figure. 2 (a)]. Positive deviation upon increasing concentration indicates that the increasing the magnitude of non-covalent interaction between the component molecules of liquid mixtures.[54-55] If the strong interactions arises among the components of a mixture leading to the formation of molecular aggregates with more compact structures, then sound will travel faster through the mixture by means of longitudinal waves and hence the positive linear behaviour of ultrasonic speed deviations will be the predominant one in **1-3** with iodine molecule. It is also noted that the excess ultrasonic velocity (u^E) value increases significantly with concentration for a given system. This shows that the extent of complex formation or halogen bonding increases with concentration of iodine and **1-3**.

Further, the excess isentropic compressibility value (κ^E) is taken account in order to understand the structural changes upon association of molecules through non-covalent interactions. The sign and magnitude in excess isentropic compressibility (κ^E) play vital role in assessing the compactness due to molecular interaction in liquid mixtures through hydrogen-bonding, charge-transfer complex formation, dipole–dipole interactions, interstitial accommodation, orientation ordering and even possible chemical effect.[31-32,49] According to Pandian et al[56], the negative excess isentropic compressibility (κ^E) values are associated with closely packed molecules through which one can account for the existence of strong molecular interaction between unlike molecules where as a positive excess values may cause dispersion forces between unlike molecules. Plots of κ^E against concentration of **1-3** with iodine are given in Figure 2 (b), From the data in Table 2 it is observed that κ^E values are negative at all concentration and also κ^E reaches a large negative value at high concentration.[31,57] This clearly indicates that the charge transfer interaction between the unlike molecules is predominant one. Similar trend is observed for excess intermolecular free length (L_f^E, Table 2) and also the trend in acoustic impedance shows non-linear increasing variation with increase in molar concentration of **1-3**.[24,58] The negative values of both κ^E and L_f^E (except **1**) also reveal the possibility of interstitial accommodation of iodine species into the void created by the aromatic molecules.[59] The positive deviation in Z^E and u^E and the negative deviation in both κ^E and L_f^E in **2** and **3** are found to be the solid evidence for the presence of strong non-covalent association through CT complex formation. But in the case of **1**, positive deviation is observed in both L_f^E and u^E

properties. However, there is negative deviation in κ^E in the investigated concentration range. Z^E values are negative at low concentration and positive at high concentration in **1**. This indicates that the CT complex formation is found to be weak in **1** when compared to **2** and **3**. The relative values of these parameters appear to be greater in **2**. This may be due to the CT complex formation is preceded after the breaking of intermolecular hydrogen bonds by the solvent molecules. In the other two ternary systems, **3** show stronger interaction than **1** as indicated by the positive values of L_f^E in **1**. This shows that the complex formation may be due to CT interaction. The trend in the acoustical and excess thermo-acoustic properties with concentration in **1-3** clearly suggests the possibility of strong solute – solute interaction and existence of charge transfer type of interaction. Structure breaking behaviour is prominent in **2** and it is clearly confirmed from the variation of acoustical properties with concentration. The order of magnitude of CT complex formation is found to be in the following order: **3 > 2 > 1**. This is also clearly confirmed through the calculation of stability constant (K) and free energy of formation ($\Delta G^{\ddagger}$) from the ultrasound velocities at different concentration using the Kannappan equation.[31] These values are listed in Table 3 along with the free energy of formation and relaxation time of these complexes. **3** is found to have higher stability constant (K) and free energy of formation ($\Delta G^{\ddagger}$) values than **1** and **2**. The calculated K values and $\Delta G^{\ddagger}$ values computed by ultrasonic method suggest that the decreasing order of stability of halogen bonded complexes is **3 > 2 > 1**. The relaxation time of the complexes (**1-3**) is of the order of femto seconds (Table 3) and they are of the same order for the three complexes indicating the formation of similar type of complex in the three systems.

3.2 UV-Vis Absorption Measurements:

In addition to the acoustical analysis, Spectrophotometric method is employed to study the nature of non-covalent interactions such as CT complexes between **1-3** and iodine molecule in n-hexane as well as aimed to correlate the stability of donor–acceptor complexes as evidenced by the acoustical parameters. The UV - visible absorption spectra of I_2 with **1-3** in n-hexane medium at 303 K with different concentration of donors (**1-3**) and keeping the concentration of iodine constant are shown in Figure S1 (a-c). It is found that the wavelength (λ_{max}) of maximum absorption for donor-acceptor interaction of iodine is found to be blue shifted as a function of the donor concentration in all the three cases (**1-3**). The sharp UV band appears at 360 nm due to the charge transfer absorption of **3** after mixing the 3 with iodine (Figure S1 (c). In the case of

1   phenol-iodine complex (Figure S1 b), the λ_{max} value for CT absorption band is observed at 270

2   nm whereas in the case of **1**, CT absorption band is found to be 260 nm (See Figure S1 (a). The

3   B-H plots drawn between the reciprocal of donor concentration ($[D]^{-1}$) to the ratio of acceptor

4   concentration with absorption ($[A]\ Abs^{-1}$) is shown in Figure 3. The excellent linear correlation

5   is obtained with correlation co-efficient of about 0.99 in all the three plots which reveals the

6   formation of 1:1 complexes in all the three systems investigated. The maximum absorption

7   values at different concentration of [D] at λ_{max} determined from the spectra were used further to

8   determine the association constant (K) and free energy of formation by Benesi – Hildebrand

9   method (B-H).[6] (Figure 3). The calculated K, $\Delta G^{\ddagger}$ values using B-H method along with λ_{max} and

10 ε are listed in Table 3. The stability constant and free energy of formation for **3** are 463.3mol^{-1}

11 and -15.5kJ mol^{-1} respectively. These values are higher than those for **1** & **2**. It may be pointed

12 out that the values obtained from B-H method excellently agree with the values obtained from

13 the acoustical parameters. It is interesting to note that the decreasing order of stability of these

14 halogen bonded complexes is **3** > **2** > **1** as established in ultrasonic, UV-Visible and B-H

15 methods.

16 **3.3 Theoretical Predictions:**

17 In order to gain deeper insights on the structural origin of the CT interaction between **1-3**

18 and iodine, DFT calculations were performed. In the case of CT complexes involving aromatic

19 system containing heteroatom, iodine atom can have two different orientations (Figure 4) i.e.

20 either through π-bonds (π-complex, a) or localized interaction through the lone pair of

21 heteroatom of the benzene (σ-complex or halogen bonding, b) as reported earlier.[60] Both the π-

22 and halogen bonded types of interaction are considered in the present study. The optimized

23 geometries along with the notable structural parameters are given in Figure 4.

24 Computed interaction energy values indicates that the formation of π-complexes (**1a-3a**)

25 is found to be energetically more favoured than the formation of halogen bonded complexes

26 through more localized interaction via heteroatom of the aromatic ring (**1b-3b**). The interaction

27 energy differences between two conformations are ranging from 6.4 to 9.2 kJ mol^{-1}. In both

28 complexes, **3** is found to have prominent ability to form the CT complexes with iodine molecule

29 than **1** and **2**. It is observed that **1a** and **3a** have largest energy differences of about 8.3 kJ mol^{-1}

30 and the least among **2a** and **3a** (about 4.7 kJ/mol). In the case of **1a** to **3a**, atom-centered

31 structure is found to be the most stable orientation. This is in contrast with the benzene-iodine

1   CT complexes where the bond-centered orientation has been shown to be the stable geometry.[18]

2   In the present study, it is clearly observed that the orientation of the iodine is largely governed by

3   the substituent present in the aromatic ring while forming CT complex. Thus in the case of **1a**,

4   iodine molecule is forming the CT complex with **1** by atom centered orientation in *para*-position

5   with respect to chloro substituent but **2a** and **3a** prefers to form atom-centered orientation in

6   *ortho* position. This is due to the site directing influence of the substituents (-OH, -OCH$_3$ and –

7   Cl) present in aromatic ring.

8   The relevant structural data for the isolated molecule and the CT complexes (both

9   halogen bonded and π-complex type) are shown in Table 4. During the formation of CT

10   complexes, the geometrical parameters are altered significantly in the I-I bond, incipient O-I

11   bond and C-C bonds of aromatic ring. The bond length of the native I-I is found to be 2.758 Å.

12   Upon forming the CT complexes with **1-3**, I-I bond is elongated largely in both **3a** (0.063 Å) and

13   **3b** (0.03 Å) and the elongation of I-I bond is found to be less in the case of **2a** (0.024 Å) and **2b**

14   (0.009 Å). In addition to that, the bond lengths of incipient C=C bond of aromatic ring are not

15   altered in **1b-3b** and it is much more elongated in **1a-3a**. It clearly shows that the involvement of

16   delocalized π-electrons forming the π-complex with iodine. Similarly C-I bond length is found to

17   be shorter in **3a** (2.979 Å) and **3b** (2.790 Å) whereas longest in **1a** (3.007 Å) and **1b** (3.148 Å).

18   The shorter X-I bond and longer I-I bond in both **3a** and **3b** clearly indicates that anisole (**3**) is

19   found to have greater tendency to form weak complexes with iodine. The variation of structural

20   parameters is found to be strongly reflected in the computed interaction energies of CT

21   complexes studied in the present work. Our computed interaction energies are in good agreement

22   with the association energies obtained from both acoustic and spectrophotometric methods.

23   **3.4 AIM analysis:**

24   To gain further insights into the nature of non-covalent interactions in these complexes,

25   Atoms in Molecules (AIM) theory[61] was used. It is based on the topological properties of the

26   electron density (ρ) estimated at the bond critical point (BCP) between two interacting atoms.[62]

27   It is well known that the appearance of (3,-1) BCP along the bond path confirms the presence of

28   bonding/nonbonding interactions.[63-64] To characterize the various non-covalent interactions,

29   Bader and co-workers have proposed a set of criteria on the computed properties at the bond

30   critical point (BCPs). The strength of the bond is often measured with the help of electron

31   density $\rho(r)$ at the BCPs, whereas the Laplacian of electron density provides information about

1   the nature of the bond. The computed topological properties are given in Table 5 and the
2   molecular graphs are given in Figure 5. From the Figure (5), it is clear that the nonbonding
3   interactions are confirmed by the presence of BCP between iodine and the interacting donor
4   molecule. It is interesting to look into the molecular graphs of **3a** and **3b**. As discussed in
5   previous analysis, **3a** is found to show two BCPs between iodine atom and the interacting carbon
6   and the hydrogen of methyl group. This is the reason why it is stabilized well over the **3b** where
7   we observe only one BCP. The value of $\rho(r)$ of 3b (0.02768 a.u) is higher than that of **3a**
8   (0.02337). But acoustic and DFT studies show that **3a** is found to be more stable. This is due to
9   the additional stabilizing H---I interaction along with C---I interactions observed in **3a** (See
10 Molecular Graph). The $\rho(r)$ is found to be 0.00705 a.u for the H---I interaction in **3a** (Table 5).
11 The value of $\rho(r)$ at the BCP of H---I interaction lies well within hydrogen bonding range (0.002-
12 0.034) with a negative L(r) value in line with earlier reports.[61,65] But this additional hydrogen
13 bonding is missing in **3b**. This synergy makes **3a** to be more stable than **3b**. Another interesting
14 property is the |V|/G ratio, a sensitive index to measure the covalency of the interactions[66]. In
15 AIM theory, the potential energy density |V| portrays the ability of the system to concentrate
16 electrons at the BCPs. But the tendency of the electrons to spread out can be estemated by the
17 kinetic energy density G.[66b] If the |V|/G < 1, then the interactions are closed-shell nature and are
18 considered to indicate a depletion of electrons at the BCPs. Accumulation of electrons at the
19 BCPs will result in |V|/G>2 which corresponds to a shared-shell interaction. i.e, a covelent bond.
20 Values of |V|/G between 1 and 2 implies that the interactions have partial covalent and partial
21 ionic character.[66a] Table 5 shows that all the pi-complexes (**1a-3a**) are found to have higher |V|/G
22 ratio values than corresponding sigma complexes (**1b-3b**). The order of covalency follows **3** > **2**
23 > **1** in both **1a-3a** and **1b-3b** systems which is again in excellent agreement with our earlier
24 analysis. It is important to note that **2a** is found to show only one interaction (C---I) whereas **2b**
25 possesses O---I & H---I interactions. But the |V|/G ratio of C---I in **2a** is 1.02989 whereas the
26 same for **2b** is 0.93797. This tells that **2a** is found to show more covalent character than **2b**.

27   Similarly, the least stable **1a** and **1b** among the three BCPs clearly substantiate the
28 existence of weak interactions between them. Further, to understand these interactions clearly
29 Laplacian of rho graphs have been drawn in Figure 6. Examination of Laplacian of rho graph of
30 **3a** indicates will give an idea as how the interacting atoms (carbon and hydrogen) tend to deform
31 its original spherical shape. The figure portrays the two types of interaction that stabilizes the **3a**;

one is C---I interaction and the other one is H---I interaction. It clearly brings out the synergy of

hydrogen bonding along with the C---I interactions. Thus our AIM topological analysis brings

insight into the nature of interactions and correctly reasons out the order of stability as well.

3.5 TD-DFT analysis:

The formation of CT complexes between donor-acceptor molecules are confirmed

through the absorption parameters such as absorption maxima (λ_{max} in nm). Notably, absorption

maxima (λ_{max} in nm) of CT bands involves the transition from π-orbital of aromatic ring) to σ^*

orbital of I-I bond is need to be considered. In this regard, we have employed TD-DFT

calculation[43] using ωB97x-D3 functional. The calculated λ_{max}, vertical transition energies (ΔE,

eV) and oscillator strengths (f), of both π and σ-type of interaction are summarized in Table 4.

Only the π-type of interaction (**1a-3a**) shows the CT transition band similar to the experimentally

observed CT band with considerable oscillator strengths, while the halogen bonded type (**1b-3b**)

does not show any kind of CT absorption band. Therefore, the interaction between iodine and

1-3 is due to the formation of π-complex type of interaction (**1a-3a**). The computed absorption

results show that the **3a** have an allowed CT band at 364 nm with oscillator strength of 0.194.

The observed experimental absorption band for **3a** is at 360 nm. It is also noted that the

calculated absorption band for **1a** and **2a** is 293 nm and 279 nm respectively with the oscillator

strength of 0.601 and 0.522. Detailed inspection of MOs in Figure 7 clearly shows that the

majority of electronic distribution of the frontier molecular orbitals were found to be transition

from $\pi_{C=C}$ $\rightarrow$ $\sigma^*(I_2)$. Our computed TD-DFT-ωB97x-D3 absorption parameters are in good

agreement with the CT band as observed in experiments. Based on our experimental and

computed TDDFT-ωB97x-D3 absorption spectra along with the acoustic parameters, atom-

centered orientation is found to be preferred for **1a-3a**.

3.6 NBO analysis:

The nature of non-covalent charge transfer interactions is often estimated by

understanding the electronic wave functions of the occupied and unoccupied non-Lewis

localized orbitals on the NBO basis.[45,67-68] The second order perturbation interaction between

donor–acceptor orbital provides useful insights on the stability of charge transfer complexes.[69] It

is well known that charge transfer interaction is largely associated with the non-zero overlap

between the benzene (donor) π-orbital and iodine (acceptor) σ^* orbital. Lower electronegativity

1　　and larger sigma hole of iodine molecule show higher stabilization interaction energy in both σ-

2　　and π- type complexes of **1-3**. Among the two types of complexes, π-type complexes (**1a-3a**) are

3　　found to have higher second order interaction energies than σ- type complexes (**1b-3b**). In the

4　　case of **3a**, $\pi_{C=C} \rightarrow \sigma^*(I_2)$ is found to be the prominent interaction leading to have stabilization

5　　energy of 44.94 kJ/mol whereas **2a** are found to have similar weak interaction energies in the

6　　order of 44.71 kJ/mol. In the case of **1a**, $\pi_{C=C} \rightarrow \sigma^*(I_2)$ is found to be the less prominent

7　　interaction by 34.01 kJ/mol (Table 4). From the Figure 8, it is observed that in **1a-3a**, the π-

8　　orbital of substituted benzene ring interact with σ* orbital of highly electrophilic iodine molecule

9　　whereas in the case of halogen bonded complexes (**1b-3b**), the interaction between lone pair of

10　　heteroatom (O atom in **2b** and **3b** and Cl atom in **1b**) and σ* orbital of iodine molecule is

11　　explained. **1b** is found to have larger interaction energy than **2b** and **3b**. The order of stabilizing

12　　interaction energies among **1a-3a** is found to be: **3a** > **2a** > **1a**. Again this is in excellent

13　　agreement with the trend observed in stability of complex formation observed by acoustic,

14　　spectrophotometric methods and DFT computed interaction energies and supports the more

15　　favourable π-type complexes (**1a-3a**) over the less favourable σ- type complexes (**1b-3b**).

16　　**Conclusions:**

17　　　　　　The nature of interactions present in three charge transfer (CT) complexes namely

18　　chlorobenzene-iodine (**1**), phenol-iodine (**2**) and anisole-iodine (**3**) have been investigated using

19　　ultrasonic, UV-Visible spectral and quantum chemical studies. Our results show that the strong

20　　solute – solute interaction and existence of charge transfer interaction present in these CT

21　　complexes. The decrease in intermolecular free length (L_f) leads to positive deviation in sound

22　　velocity (u) and negative deviation in isentropic compressibility(κ_s) in **1-3.** Among the three CT

23　　complexes, the structure-breaking property of intermolecular hydrogen bonded phenol is

24　　predominant in **2** prior to the CT complex formation with Iodine. This has been confirmed by the

25　　negative deviation in the speed of sound in very dilute solution. Ultrasonic studies reveal that the

26　　order of magnitude of CT complex formation is **3** > **2** > **1** and this trend is confirmed by the

27　　stability constant (K) and free energy of formation ($\Delta G^{\ddagger}$) from Benesi-Hildebrand method. DFT

28　　studies portray that the π-type complex is found to be energetically more favourable than the

29　　halogen bonded complex and atom-centered orientation is found to be the preferred geometry.

30　　AIM and NBO analysis corroborate the predicted DFT results which in turn well agree with

31　　experimental findings. TDDFT results show that $\pi \rightarrow \sigma^*$ transitions are responsible for the charge

1 transfer nature of these CT complexes. In summary, it is established that acoustic method can be

2 employed as a simple and non-destructive tool to characterize the charge transfer non-covalent

3 interactions present in these CT complexes. The computed results are in good agreement with the

4 experimental observations. Further the orientation of iodine molecule depends on the substituent

5 present in the aromatic ring. A further study on the influence of different types of substituent in

6 the aromatic ring on the orientation of iodine molecule is underway in our laboratory.

7

8 **Electronic supplementary information (ESI) available.**

9 The corresponding UV-Visible spectrum for 1-3 with I_2 and optimized geometries of all of the

10 molecules along with their XYZ coordinates.

11

12 **AUTHOR INFORMATION**

13 Corresponding Author
14 *Tel.: 91-44-28178200. Fax: +91-44-28175566
15 E-mail: madhavanjack05@gmail.com

16

17 **ACKNOWLEDGEMENTS:**

25

26 **REFERENCES:**

27 1. D. S. Reddy, D. C. Craig, G. R. Desiraju, *J. Am. Chem. Soc.* 1996, **118**, 4090–4093.
28 2. a) Y. X. Lu, Y. Wang, W. L. Zhu, *Phys. Chem. Chem. Phys.* 2010, **12**, 4543–4545.; b) K. S.
29   Yeung, *Drug Discovery Today*, **2011**, **15**, 158.
30 3. F. Yakuphanoglu, M. Arslan, *Physica B: Condensed Matter*, 2007, **393**, 304 - 309.
31 4. a) F. Yakuphanoglu, M. Arslan, *Solid State Commun.* 2004,**132**, 229 - 234.;
32 5. F. Guthrie, XXVIII. *J. Chem. Soc.* 1863, *16*, 239-244.
33 6. H. A. Benesi, J. H. Hildebrand, *J. Am. Chem. Soc.* 1949, **71**, 2703-2707.
34 7. R. S. Mulliken, W. B. Pearson, Molecular Complexes. Wiley Publishers, New York, 1969.
35 8. R. S. Mulliken, *J. Am. Chem. Soc.* 1950, **72**, 600.

9.   J. Collin, L. D'Or, *J. Chem. Phys*. 1955, **23**, 397.

10. H. Bai, B. S. Ault, *J. Phys. Chem*. 1990, **94**, 199.

11. Hassel, O. Strømme, K. *Acta Chem. Scand*. 1958, **12,** 1146.

12. L. Fredin, B. Nelander, *J. Am. Chem. Soc*. 1974, **96**, 1672-1673.

13. L. Fredin, B. Nelander, *Mol. Phys*. 1974, **77**, 885-898.

14. E. E. Ferguson, *J. Chem. Phys*. 1956, **25**, 577-578.

15. E. E. Ferguson, *Spectrochim. Acta.* 1957, **10**, 123-124.

16. J. C. Shug, M. C. Dyson, *J. Chem. Phys*. 1973, **58**, 297.

17. R. E. Bruns, *J. Mol. Struct.* 1977, **36**, 121-126.

18. A. M. Mebel, H. L. Lin, S. H. Lin, *Int. J. Quantum Chem*.1999, **72**, 307-318.

19. K. Weng, Y. Shi, X. Zheng, D. L. Phillips, *J. Phys. Chem. A* 2006**, 110***,* 851-860.

20. S. S. C. Ammal, S. P. Ananthavel, P. Venuvanalingam, M. S. Hegde, *J. Phys. Chem. A* 1998, **102**, 532-536.

21. A. K. Nain, *J. Chem. Thermodynamics*, 2013, **59**, 49–64.

22. T. Zhao, J. Zhang, L. Li, B. Guo, L. Gao, X. Wei, *J. Mol. Liq*. 2014, **198,** 21–29.

23. D. L. Cunha, J. A. P. Coutinho, J. L. Daridon, R. A. Reis, M. L. L. Paredes, *J. Chem. Eng. Data,* 2013, **58**, 2925–2931.

24. A. Ali, A. K. Nain, V. K. Sharma, S. Ahmad, *Phys. Chem. Liq*. 2004, **42**, 375–383.

25. R. Kumar, S. Jayakumar, V. Kannappan, *Fluid Phase Equilibria,* 2013, **360**, 309– 319.

26. R. Kumar, G. Padmanabhan, V. Ulagendran, V. Kannappan, S. Jayakumar, *J. Mol. Liq.* 2011, **162,** 141–147.

27. R. Kumar, A. Justin Adaikala Baskar, V. Kannappan, D. Roop Singh, *J. Mol. Liq.* 2014, **196,** 404–410.

28. R. Kumar, S. Jayakumar, V. Kannappan, *Thermochimica. Acta.* 2012, **536**, 15–23.

29. S. R. Salman, S. J. Titinchi. H. S. Abbo. A. A. Saeed. *Spectroscopy Letters*, 1990, **23**, 447-457.

30. E. Y. Frag, G. G. Mohamed, *J. Mol. Struc*. 2010, **979**, 46 –55.

31. a) V. Ulagendran, R. Kumar, S. Jayakumar, V. Kannappan, *J. Mol. Liq*. 2009, **148**, 67-72.; b) V. Kannappan, N. Indra Gandhi, *Phys. Chem. Liq.,* 2008, **46**, 510-515.

32. F. C. Küpper and P. M.H. Kroneck, Iodine Bioinorganic Chemistry, ed. T. Kaiho, John Wiley & Sons Interscience, 2015, Ch.32, pp 555-589.

33. B. L. Merwein, S. N. Bhat, *Thermochimica Acta*, 1987, **118,** 277–285.

34. M. J. Frisch, G. W. Trucks, H. B. Schlegel, G. E. Scuseria, M. A. Robb, J. R.Cheeseman, G. Scalmani, V. Barone, B. Mennucci, G. A. Petersson, H. Nakatsuji, et al. Gaussian 09, Revision B.01; Gaussian, Inc.: Wallingford, CT, 2009.

35. F. Neese, Density Functional and Semi empirical Program Package, version 2.8, University of Bonn, Bonn, Germany, 2009.

36. J. P. Perdew, W. Yue, *Phys. Rev. B*, 1986, 33, 8800–8802.

37. D. Becke, *Phys. Rev*., 1988, 3098–3100.

38. S. Grimme, J. Antony, S. Ehrlich, H. Krieg, *J Chem. Phys*. 2010, *132*, 15104.

39. a) C. Lee, W. Yang, R. G. Parr, *Phys. Rev. B*, 1988, *37*, 785–789. b) D. Becke, *J. Chem. Phys*., 1993, *98*, 5648–5652.

40. D. A. Pantazis, F. Neese*, Theo. Chem. Acc*. 2012, **131**, 1292.

41. S. F. Boys, F. Bernardi, *Mol. Phys*. 1970, **19**, 553–557.

42. A. Klamt, *G. J. Schüürmann, Chem. Soc*. *Perkin Trans*. *2*: 1993**,** 799–805.

43. A. Dreuw, M. Head-Gordon, *Chem. Rev*. 2005, **105**, 4009−4037.

44. E. Glendening, A. Reed, J. Carpenter, F. Weinhold, NBO; University of Wisconsin: Madison, WI, 1998.
45. A. E. Reed, L. A. Curtiss, F. Weinhold, *Chem. Rev.* 1988, **88,** 899−926.
46. J. −D. Chai, M. Head-Gordon, *Phys. Chem. Chem. Phys.*, 2008, **10**, 6615–6620.
47. a) J. M. L. Martin, A. Sundermann, *J. Chem. Phys.* 2001, **114**, 3408-3420.; b) J. Tomasi and M. Persico, Chem. Rev., 1994, 94, 2027.; c) J. Tomasi and R. Cammi, J. Comput. Chem., 1995, 16, 1449.; d) M. Cossi, V. Barone, R. Cammi and J. Tomasi, Chem. Phys. Lett., 1996, 255, 327.
48. F.Biegler-König, J. Schönbohm, D. Bayles, AIM2000. *J. Comput. Chem.* 2001, **22,** 545−559.
49. A. Awasthi, M. Rastogi, M. Gupta, J. P. Shukla, *J. Mol. Liq.* 1999, **80**, 77.
50. B. D. Nageshvara Rao, P. V. Venkatesawaralu, A. S. N. Murthy, C.N.R. Rao *Canadian J. Chem.* 1962, **40**, 963-965
51. L. Palaniappan, *Physica B,* 2008, **403**, 3887–3891.
52. S. L. Oswal, V. Pandiyan, B. Krishnakumar, P. Vasantharani, *Thermochimica Acta*, 2010, **27**, 507–508.
53. R. Thiyagarajan, M. S. Jaafar, L. Palaniappan, *J. Phys. Sci.* 2007, **18**, 81–88.
54. B. Dalai, S. K. Dash, S. K. Singh, *Ind. J. Pure Appl. Phys.* 2014, **52**, 24-29.
55. Y. Reddy, P. S. Naidu, K. Ravindra Prasad, *Indian J. Pure Appl. Phys.* 1994, **32,** 958–963.
56. V. Pandiyan, S. L. Oswal, P. Vasantharani, *Thermochimica Acta*, *2011*, **516,** 64–73.
57. R. J. Fort, M. W. R. Moore, *Trans. Faraday Soc. 1*965, **61**, 2102-2111.
58. R. R. Naik, S. V. Bawankar, *African J. Sci. Research,* 2014, **3**, 1-3.
59. A. Ali, A. K. Nain, *Bullet. Chem. Soc. Japan*, 2002, **75**, 681–687.
60. C. Wang, D. Danovich, Y. Mo, S. Shaik, *J. Chem. Theory Comput.* 2014, **10**, 3726–3737.
61. R. F. Bader, W. *Chem. Rev.* 1991, **91**, 893-928.
62. R. F. Bader, *J. Phys. Chem. A.* 2009, **113**, 10391-10396.
63. R. Vijay Solomon, S. A. Vedha, P. Venuvanalingam, *Phys. Chem. Chem. Phys.* 2014, **16,** 7430-7440.
64. M. Sundararajan, R. Vijay Solomon, S. K. Ghosh, P. Venuvanalingam, *RSC adv.* 2011, **1**, 1333-1341.
65. A. Mohajeri, F. F. Nobandegani, *J. Phys. Chem. A* 2008, **112**, 281-295.
66. E. Espinosa, I. Alkorta, J. Elguero, Molins, E. *J. Chem. Phys.* 2002, **117**, 5529-5542. 67.; b) Espinosa, E., Molins, E. and C. Lecomte, *Chem. Phys. Lett*. 1998, **285**,170–173.
67. A. E. Reed, F. Weinhold, *J. Chem. Phys.*, 1985, **83**, 1736-1741.
68. W. Wang, N. B. Wong, W. Zheng, A. Tian, *J. Phys. Chem. A*, 2004, **108**, 1799-1805.
69. R. Vijay Solomon, P. Veerapandian, S. Angeline Vedha, P. Venuvanalingam, *J. Phys. Chem. A*. 2012, **116,** 4667−4677.

1 **Table 1**. Measured values of ultrasonic velocity (u), density (ρ) and coefficient of viscosity (η)

2 for the ternary systems 1 to 3 with iodine in n – hexane at 303K.

C (mol dm^{-3})	Chlorobenzene-I$_2$			Phenol-I$_2$			Anisole-I$_2$		
	u (ms^{-1})	ρ (kgm^{-3})	η X 10^{-4} (Nsm^{-2})	u (ms^{-1})	ρ (kgm^{-3})	η X 10^{-4} (Nsm^{-2})	u (ms^{-1})	ρ (kgm^{-3})	η X 10^{-4} (Nsm^{-2})
0.002	1066.6	645.6	4.81	1064.5	655.2	4.17	1066.2	653.6	3.80
0.004	1067.5	646.3	4.83	1065.1	657.1	4.22	1067.1	654.0	4.02
0.006	1068.2	648.0	4.83	1066.3	658.1	4.24	1067.4	655.0	4.02
0.008	1068.6	648.8	4.84	1066.8	660.6	4.24	1068.1	655.7	4.03
0.01	1069.6	651.5	4.84	1067.5	663.6	4.27	1068.4	656.0	4.04
0.012	1070.3	652.6	4.86	1068.4	665.0	4.30	1069.2	657.4	4.05
0.014	1071.4	653.3	4.86	1069.8	666.8	4.31	1070.6	658.5	4.05
0.016	1072.7	656.7	4.87	1070.8	667.9	4.33	1071.7	658.7	4.09
0.018	1074.0	656.9	4.88	1071.8	668.3	4.35	1072.3	659.3	4.10
0.020	1075.6	658.2	4.89	1072.4	668.8	4.66	1073.4	660.2	4.16

3

4

1

2 **Table 2.** The values of isentropic compressibility (κ), free length (L_f), internal pressure (π_i) and
3 acoustic impedance (Z) along with their excess values includes velocity (u^E) for ternary systems
4 1 to 3 with iodine in n – hexane at 303K.

C mol dm^{-3}	κ X 10^{-9} (kg^{-1} ms^{-2})	L_fX 10^{-11} (m)	π_i X 10^5 (atm)	Z X 10^5 (kg m^{-2}s^{-1})	Excess acoustical parameters			
					κ^E X 10^{-9} (pa^{-1})	$L_f{}^E$ X 10^{-11} (Å)	Z^E X 10^3 (kg m^{-2}s^{-1})	u^E (ms^{-1})
Chlorobenzene-I$_2$								
0.002	1.361	7.379	2.884	6.885	-0.318	0.066	-1.433	2.0
0.004	1.357	7.369	2.889	6.899	-0.656	0.062	-1.930	2.8
0.006	1.352	7.355	2.891	6.921	-1.120	0.061	-1.613	3.3
0.008	1.349	7.347	2.894	6.933	-1.342	0.060	-2.349	3.6
0.01	1.341	7.325	2.899	6.968	-2.090	0.057	-0.741	4.4
0.012	1.337	7.314	2.905	6.984	-2.440	0.056	-0.962	5.0
0.014	1.333	7.303	2.904	6.999	-2.802	0.055	-1.355	6.0
0.016	1.323	7.275	2.913	7.044	-3.763	0.052	1.240	7.1
0.018	1.319	7.265	2.913	7.055	-4.066	0.051	0.437	8.3
0.020	1.313	7.247	2.915	7.080	-4.677	0.049	1.040	9.7
Phenol-I$_2$								
0.002	1.346	7.339	2.715	6.975	-1.793	-4.799	7.440	-0.1
0.004	1.341	7.324	2.734	6.999	-2.277	-6.048	7.912	0.3
0.006	1.336	7.311	2.740	7.017	-2.719	-7.185	7.778	1.3
0.008	1.330	7.294	2.744	7.047	-3.279	-8.650	8.772	1.6
0.01	1.322	7.272	2.760	7.084	-4.023	-10.62	10.59	2.1
0.012	1.317	7.258	2.771	7.105	-4.451	-11.73	10.71	2.7
0.014	1.310	7.239	2.775	7.133	-5.090	-13.42	11.65	3.9
0.016	1.305	7.227	2.782	7.151	-5.481	-14.44	11.45	4.7
0.018	1.302	7.217	2.786	7.163	-5.755	-15.13	10.69	5.5
0.020	1.300	7.211	2.883	7.172	-5.942	-15.58	9.664	5.9
Anisole-I$_2$								
0.002	1.345	7.336	2.586	6.969	-1.907	-5.111	6.877	1.7
0.004	1.342	7.328	2.658	6.979	-2.136	-5.668	5.892	2.3
0.006	1.339	7.320	2.658	6.992	-2.369	-6.236	5.280	2.4
0.008	1.336	7.311	2.661	7.004	-2.639	-6.905	4.556	3.0
0.01	1.335	7.308	2.662	7.008	-2.695	-6.989	3.060	3.0
0.012	1.330	7.294	2.667	7.029	-3.142	-8.149	3.276	3.7
0.014	1.324	7.279	2.666	7.05	-3.645	-9.462	3.430	4.9
0.016	1.321	7.270	2.677	7.059	-3.905	-10.10	2.403	5.8
0.018	1.319	7.263	2.679	7.069	-4.100	-10.57	1.493	6.2
0.020	1.314	7.251	2.698	7.086	-4.497	-11.60	1.249	7.1

5

6

1

Table 3. Stability constant K, free energy of formation $\Delta G^{\ddagger}$, relaxation time τ (ultrasonic method), wavelength of maximum absorption λ_{max} and molar extinction coefficient ε (spectroscopic method) for CT complexes of with iodine with substituted benzenes in n-hexane at 303 K.

Donor	Ultrasonic Technique			Spectrometric Technique			
	K (mol^{-1})	$\Delta G^{\ddagger}$ ($kJ\ mol^{-1}$)	τ X 10^{-14} (s)	K (mol^{-1})	$\Delta G^{\ddagger}$ ($kJ\ mol^{-1}$)	λ_{max} (nm)	ε, $cm^{-1}\ M^{-1}$
1	56.59	-10.168	0.5319	53.76	-10.039	260	2.1 x10^5
2	379.2	-14.961	0.7830	373.5	-14.923	270	2.7x10^5
3	467.0	-15.486	0.7730	463.3	-15.466	360	2.9 x 10^4

6

Table 4. Notable structural parameters, interaction energies (kJ/mol), amount of charge transferred (q_{CT}), occupancy values in a.u, second order interaction energies (kJ/mol) and computed TDDFT parameters of of 1a-3a and 1b-3b.

Parameter	I_2	π-complexes (X=C)			σ-complexes (X=Cl, OCH_3, OH)		
		1a	2a	3a	1b	2b	3b
I-I	2.758	2.782	2.797	2.821	2.767	2.761	2.791
X-I	-	3.007	2.933	2.979	3.148	2.801	2.790
X-I-I	-	176.5	173.9	176.4	175.2	179.2	175.7
ΔE_{int}	-	-24.2	-28.9	-32.5	-17.8	-19.7	-25.1
NBO Analysis							
q_{CT}	0.000	0.131	0.142	0.146	0.010	0.110	0.083
Occupancy (au)							
$\pi_{C=C}$		1.657 1.640 1.663	1.686 1.632 1.683	1.699 1.696 1.640	1.657 1.688 1.658	1.684 1.665 1.673	1.683 1.675 1.692
$\sigma^*(I_2)$		0.058	0.080	0.082	0.050	0.036	0.048
$\Delta E^{(2)}$							
$\pi_{C=C} \rightarrow \sigma^*(I_2)$	-	34.41	44.71	44.94	-	-	-
$n_{lp} \rightarrow \sigma^*(I_2)$	-	-	-	-	43.04	35.33	38.51
TDDFT Parameters							
λ_{max}	-	293	279	364	-	-	-
f	-	0.601	0.522	0.194	-	-	-
$\Delta E(eV)$	-	4.22	4.44	3.40	-	-	-

10

11

12

Table 5. Computed AIM topological parameters for 1a-3a and 1b-3b.

System	BCP	$r(\rho)$	L(r)	ELLIPTICITY	V/G
1a	C---I	0.019	-0.01118	0.21752	0.97835
2a	C---I	0.023	-0.01166	0.12748	1.02989
3a	C---I	0.024	-0.01171	0.14604	1.03959
	H---I	0.007	-0.00469	0.24790	0.81361
1b	Cl---I	0.019	-0.01351	0.08433	0.90584
2b	O---I	0.021	-0.01639	0.13228	0.93797
	H---I	0.007	-0.00473	0.05837	0.79734
3b	O---I	0.028	-0.01915	0.08740	1.00257
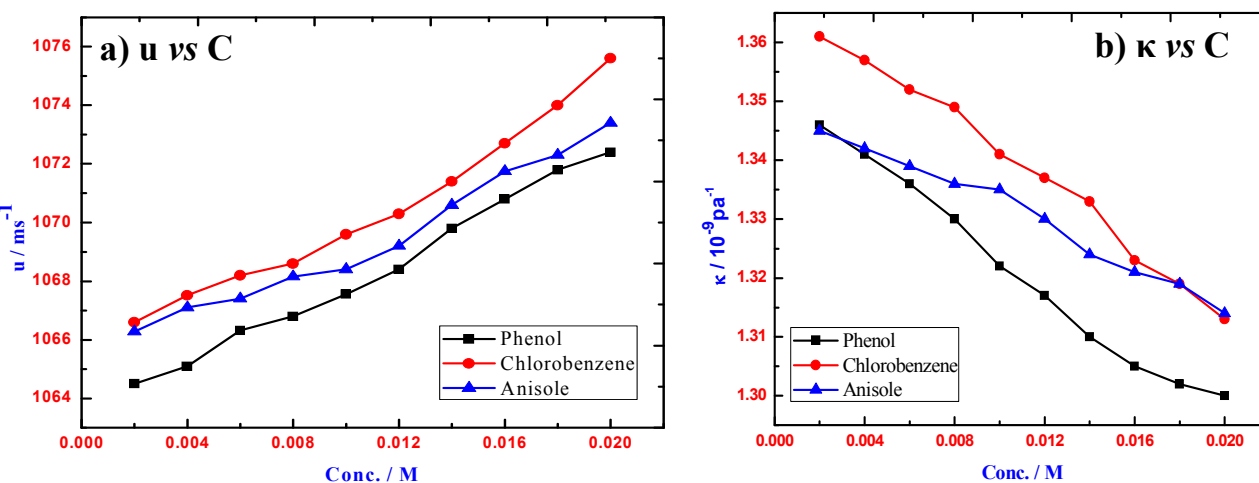
Figure 1. Plots of (a) Ultrasonic velocity versus concentration, (b) isentropic compressibility versus concentration for the three ternary systems of 1-3 with Iodine molecule in n − hexane at 303 K.
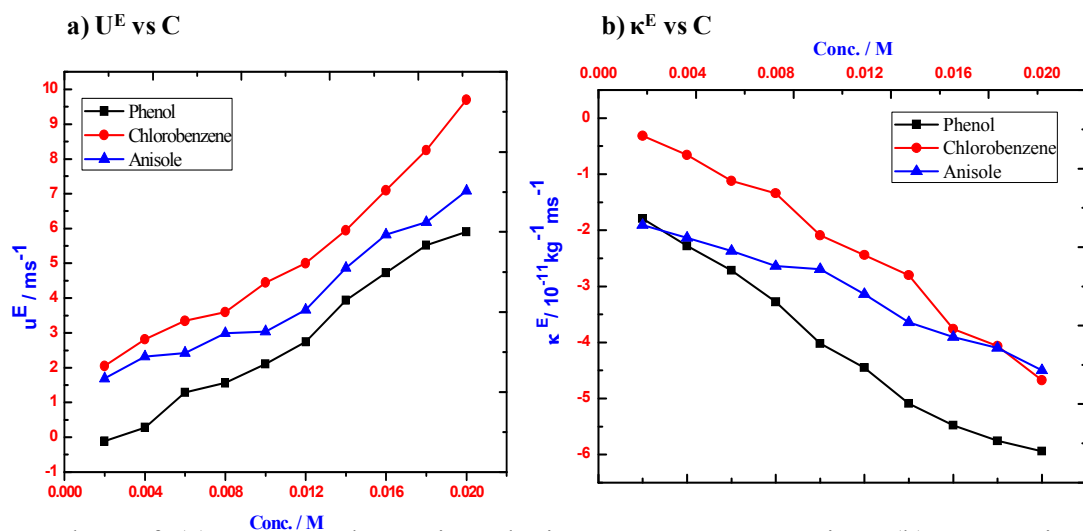
1

2

a) U^E vs C

b) κ^E vs C

Figure 2.Plots of (a) excess Ultrasonic velocity versus concentration, (b) excess isentropic compressibility versus concentration for the three ternary systems of 1-3 with Iodine in n – hexane at 303K.
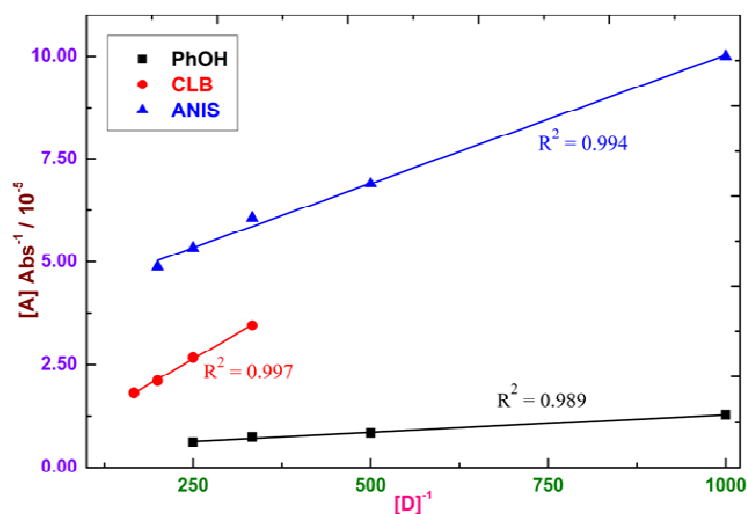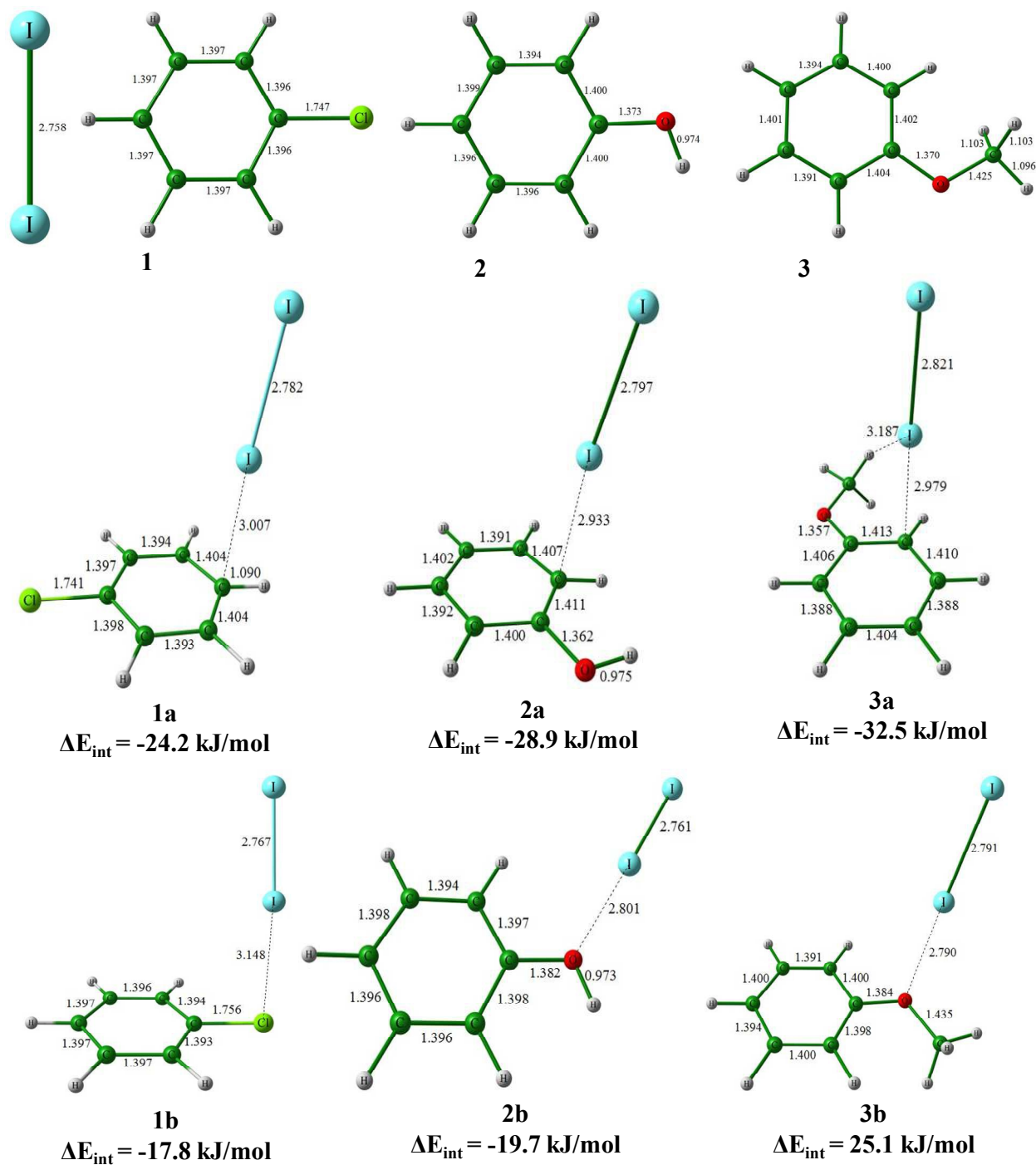

Figure 3. Benesi – Hildebrand plots for (a) chlorobenzene – I_2 (b) anisole – I_2 and (c) phenol – I_2 system in n-hexane at 303 K.

1

2

3 **Figure 4**.Optimized geometries of 1a-3a and 1b-3b along with stabilization energies and notable
4 structural parameters (Bond lengths are in Å and bond angles are in degrees º).

5

1

2

3

4

5

6

7

8

9

10

11

12

13

14

15

16

17

18

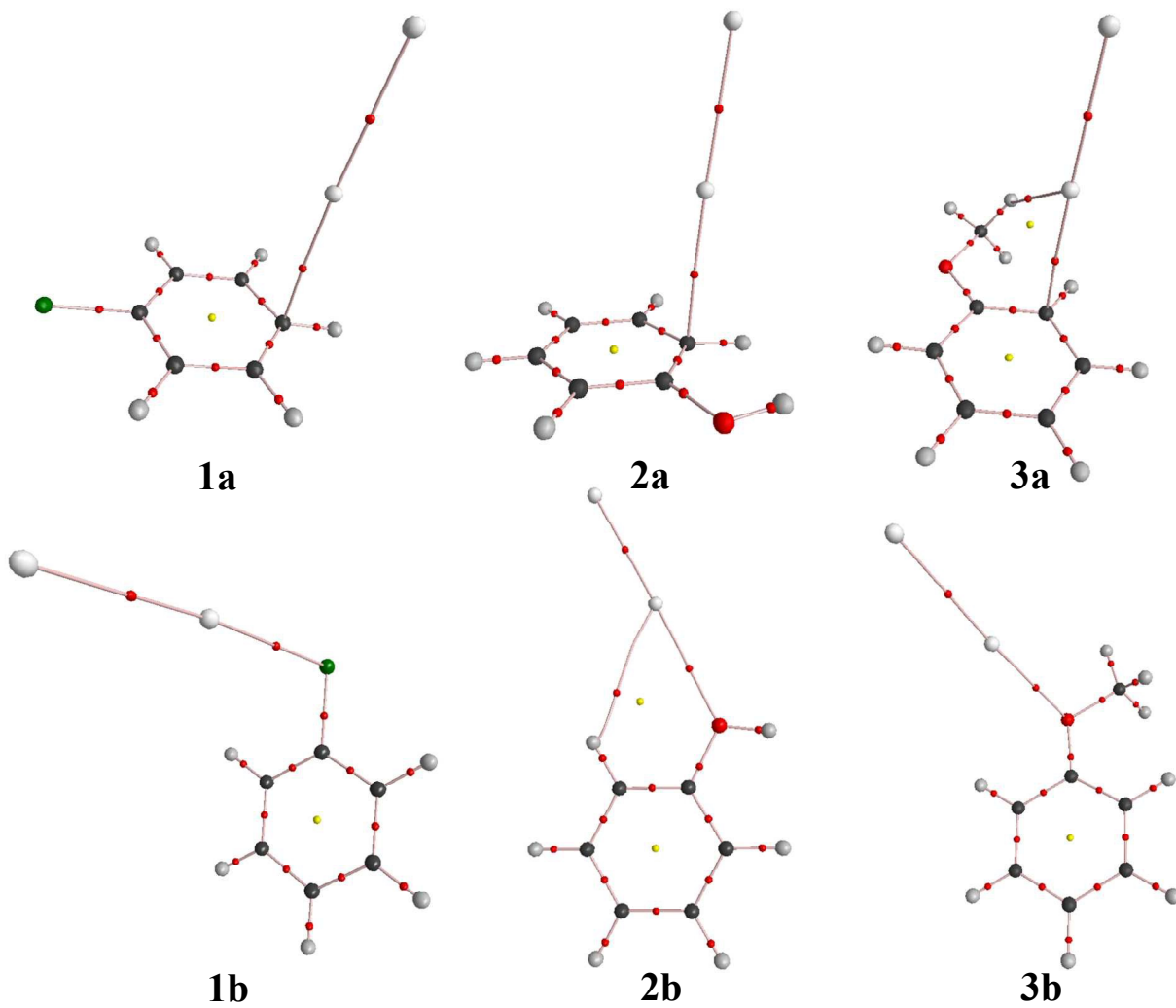19

20

21

1a　　　　　**2a**　　　　　**3a**

1b　　　　　**2b**　　　　　**3b**

22 **Figure 5**. Molecular Graphs of 1a-3a and 1b-3b.

23

24

25

1

2

3

4

5

6

7

8

9

10

11

12

13

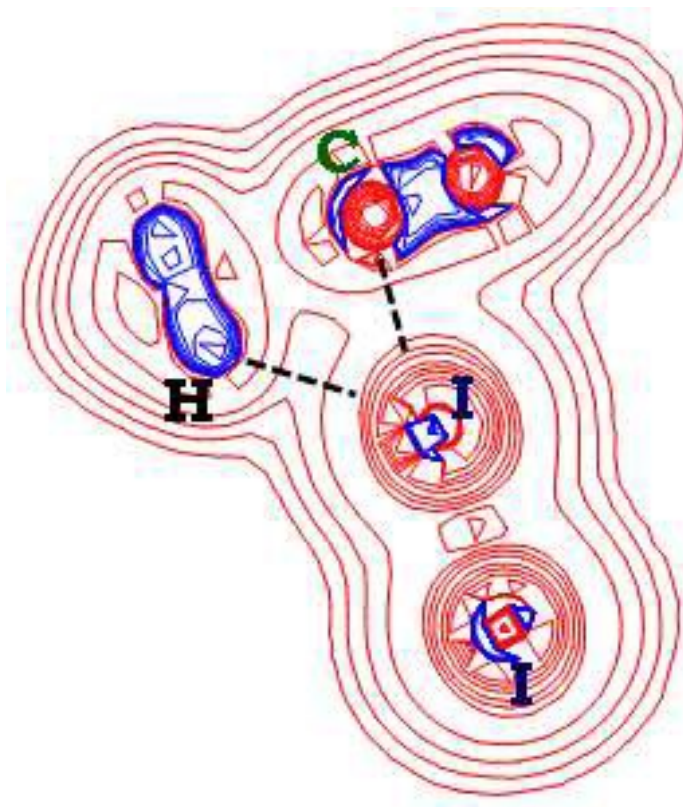14

15

16

17

18

19

20

21

22

23
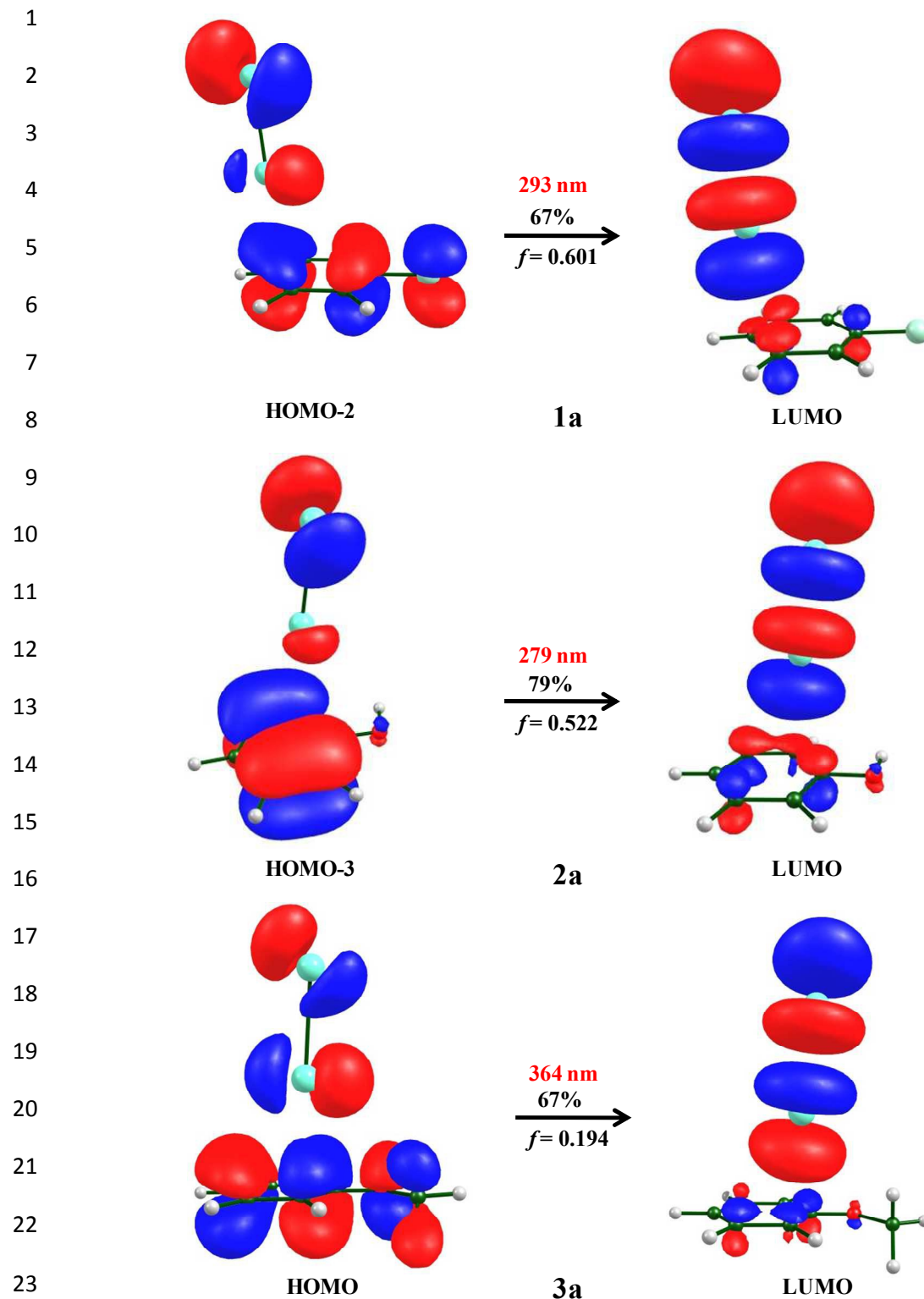
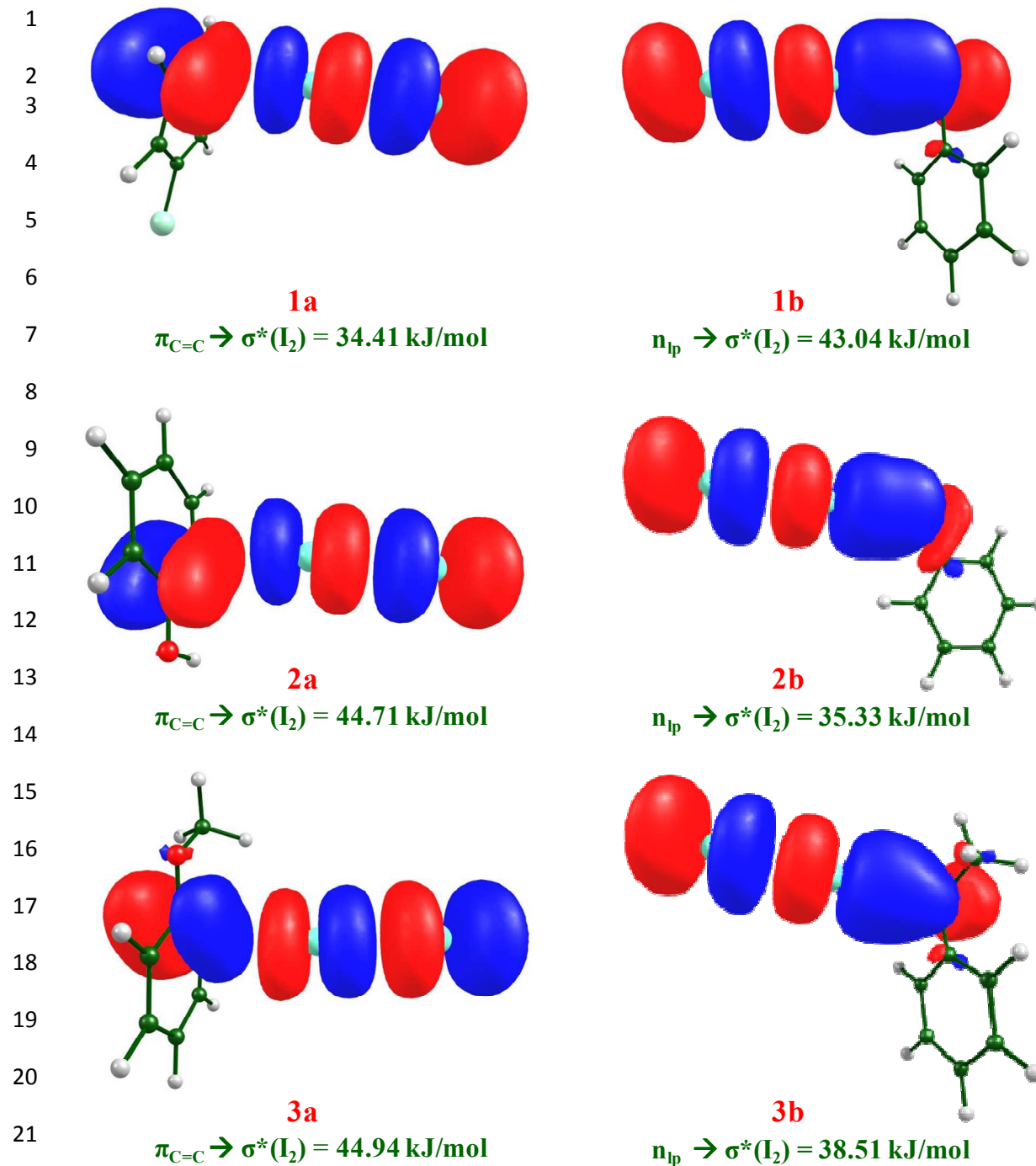24

25

26

27

28 **Figure 6**. Laplacian and rho graphs of 3a.

29

1
2
3
4
5
6
7
8
9
10
11
12
13
14
15
16
17
18
19
20
21
22
23
24
25
26

Figure 7. Frontier molecular orbitals of most prominent absorption of 1a-3a along with computed absorption maxima (λ_{max}) and oscillator strength (f)

1a

$\pi_{C=C} \rightarrow \sigma^*(I_2) = 34.41$ kJ/mol

1b

$n_{lp} \rightarrow \sigma^*(I_2) = 43.04$ kJ/mol

2a

$\pi_{C=C} \rightarrow \sigma^*(I_2) = 44.71$ kJ/mol

2b

$n_{lp} \rightarrow \sigma^*(I_2) = 35.33$ kJ/mol

3a

$\pi_{C=C} \rightarrow \sigma^*(I_2) = 44.94$ kJ/mol

3b

$n_{lp} \rightarrow \sigma^*(I_2) = 38.51$ kJ/mol

Figure 8. NBO computed orbital interactions corresponding to 1a-3a and 1b-3b of a) $\pi_{C=C} \rightarrow \sigma^*(I_2)$ b) $n_{lp} \rightarrow \sigma^*(I_2)$. Second order interaction energies are present in kJ/mol.